03,11

Impedance spectroscopy and low-frequency noise in thin films of carbon quantum dots

© G.V. Nenashev, A.M. Ivanov, P.A. Aleshin, R.S. Kryukov, A.N. Aleshin¶

Ioffe Institute,
St. Petersburg, Russia

¶ E-mail: aleshin@transport.ioffe.ru

Received June 4, 2024
Revised June 4, 2024
Accepted June 6, 2024

The results of studies of the dependences of current on applied voltage, low-frequency noise and impedance characteristics in thin films based on carbon quantum dots (CQDs) obtained from L-Lysine using microwave technology, which allows the synthesis of CQDs with an average size of less than 10 nm, are presented. The impedance spectroscopy results show that the Cole-Cole plots are in good agreement with the equivalent circuit model and represent the series resistance, recombination resistance, and geometric capacitance, respectively, which arise from charge storage, charge transfer resistance, and/or additional interfacial electronic states. The mechanisms of current flow, the formation of current noise, and the occurrence of defects are considered. In the frequency range under study ($f \leq 8000$ Hz), the $1/f$ noise associated with fluctuations in the charge carrier density is most clearly visible. A possible mechanism responsible for the transport of charge carriers in CQDs films is discussed. The results obtained make it possible to predict the properties of optoelectronic devices based on CQDs.

Keywords: carbon quantum dots, impedance spectroscopy, low-frequency noise, electrical conductivity.

DOI: 10.61011/PSS.2024.07.58990.146

1. Introduction

Carbon quantum dots (CQDs) are nanoscale particles having unique physico-chemical properties, which make them prospective materials for a wide spectrum of applications in biomedicine [1–3]. CQDs are also studied for use in the area of renewable power sources, solar cells and photoelectroplating [4,5]. Moreover, they are promising for optical and chemical sensing of exact molecules or ions [6], and as delivery systems able to encapsulate and selectively deliver therapeutic agents into the human body [7]. First discovered at the beginning of 2000s, CQDs attracted significant attention due to low toxicity, high biocompatibility and the diversity of synthesis methods. Unlike traditional semiconductor quantum dots, the carbon analogues can be made of accessible and ecologically safe initial materials, such as carbon nanotubes, graphene and carbon nanoparticles. Note that during the last period active studies of the optical and electrical properties of CQDs and their composites are performed [8,9].

The study of noise and impedance characteristics of CQDs films is an important direction to understand their behaviour under different operation conditions and optimization of their operation in actual applications.

The noise characteristics ensure understanding of fluctuations in the electric signals which can occur as result of various physical processes such as recombination of charge carriers, surface defects and interaction with the environment [10–13]. Density measurements of low-frequency current noise present data to determine nature of the frequency spectrum in optoelectronic devices, possible localization of noise sources in studied structures [14]. Analysis of these characteristics ensure the determination of key mechanisms affecting the stability and reliability of devices based on CQDs. Note that noise characteristics of CQDs films are insufficiently studied currently.

The impedance characteristics, in turn, provides the possibility to study the dynamic properties of CQDs, including conductivity and capacity effects. The impedance study allows for the understanding how materials behave at different frequencies of applied electric field, which is particularly important for the development of high-frequency devices and sensors. The impedance spectroscopy (IS), as an analysis method, provides valuable information on processes of charge transfer in materials thus facilitating the improvement of their properties for specific applications.

In the present study we provide the comprehensive analysis of noise characteristics of thin films based on carbon quantum dots, obtained from L-Lysine using microwave technology [15]. Carrier transport and mechanisms of noise formation are discussed. The IS results show that the Cole — Cole plots are in good agreement with the equivalent scheme model. The physical mechanisms of current flow, current noise formation, and defect occurrence are considered. It is identified that in the studied frequency range ($f \leq 8000$ Hz) the flicker-noise is the main, it is associated with density oscillations of charge carriers (holes and ions) in CQDs films. Mechanisms responsible for charge carriers transport in CQDs films are discussed.

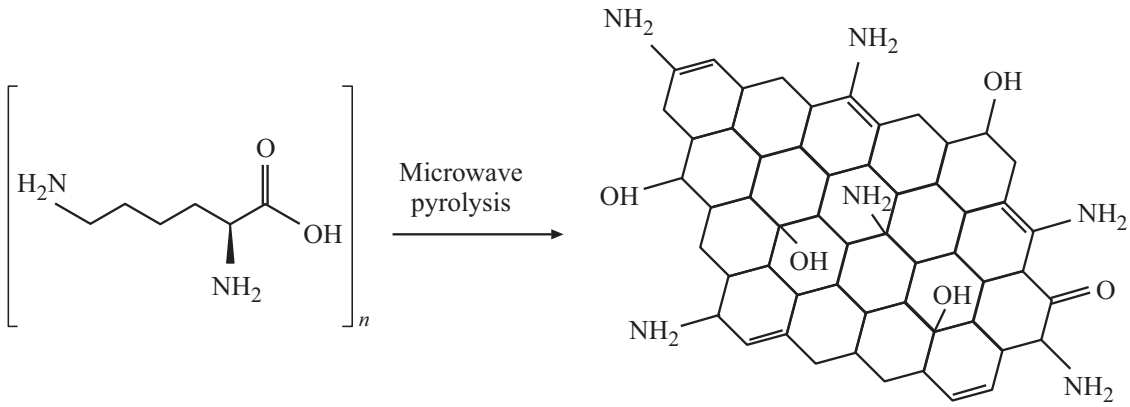

Figure 1. The process of CQD formation from L-Lysine during microwave pyrolysis [16].

2. Objects and methods of the study

The carbon nanoparticles were synthesized using a single stage method of microwave pyrolysis, from precursor L-Lysine (Sigma-Aldrich) in the amount of 1 g L-Lysine was mixed with 10 ml of distilled water and agitated using magnetic agitator for 10 min to ensure complete dissolving. The obtained solution was then relocated into a flask with round bottom, and loaded inside the consumer microwave oven heated for 5 min at a power of 650 W. During pyrolysis the solution changes color from colorless to dark-brown, major part of water evaporated. After the product cooling to room temperature, 10 ml of water was poured into vessel, then the solution was filtered using centrifuge-concentrator (Vivaspin, Sartorius) with membrane 300 kDa. Powder of carbon nanoparticles was obtained by lyophilization at a pressure 3 Pa and $-50\,^{\circ}$C for four days.

Figure 1 shows the chemical process of CQDs formation from L-Lysine by method of pyrolysis in a microwave oven.

CQDs size was determined using analyzer Zetasizer Nano ZS (model ZEN3600, Malvern Instruments, United Kingdom). According to the obtained data the average size of particles is from 1 to 30 nm at maximum of dimensions distribution in range of values 4 nm (distribution of CQDs particles by dimensions is shown in Figure 2, *a*)

To study electronic properties of CQDs they were deposited as films on glass substrate with electrodes of indium and tin oxide (ITO) (Sigma Aldrich). The distance between the flat ITO electrodes is 200 μm, and their width is about 5 mm. The current-voltage curves (I-Vs) of the samples were measured in planar geometry using a two-probe pattern at room temperature in darkness using an automated measuring set-up based on the Keithley 6487 picoammeter. The applied voltage varied from -4 to 4 V with variable pitch. The contacts to the ITO electrodes were attached with silver wire using carbon paste.

A set of measurements using impedance spectroscopy was carried out in the darkness using Elins Z-500PX impedance meter in accordance with the technique described in our previous paper [17]. The experiments were

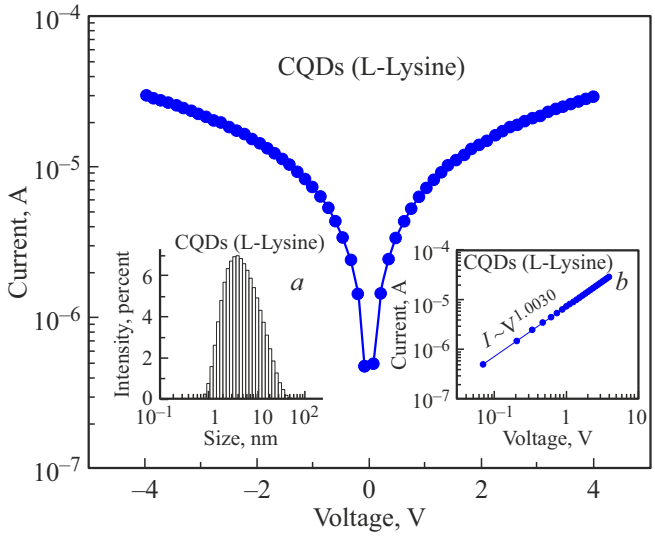

Figure 2. I-Vs of CQDs film based on L-Lysine. In inserts: *a*) distribution of dimensions of CQDs based on L-Lysine; *b*) I-Vs of same CQDs film based on L-Lysine in lg – lg scale.

carried out at a forward bias from 0 to 1 V and in the frequency range from 10 Hz to 0.5 MHz. Results obtained from measuring IS were processed using licensed software Z-View. To minimize external interference, samples were placed in a metal insulated box.

Densities of current noise and voltage fluctuations were measured in a frequency band of 7.3 kHz and by passing direct current via CQDs film based on L-Lysine and registration of voltage fluctuations on the loading resistor $R = 100\,\Omega$. Spectral and noise characteristics of samples were measured using semi-automatic unit [17], based on analog-to-digital converter STC-H246 Kamerton with own level of noises 1 μV, at that $2 \cdot 10^6$ samples with sampling rate of 16 kHz were put in the computer memory. According to the sample data the noise spectrum was calculated using fast Fourier transform in four bands of same width 17.6 Hz. Program of processing the registered spectra calcu-

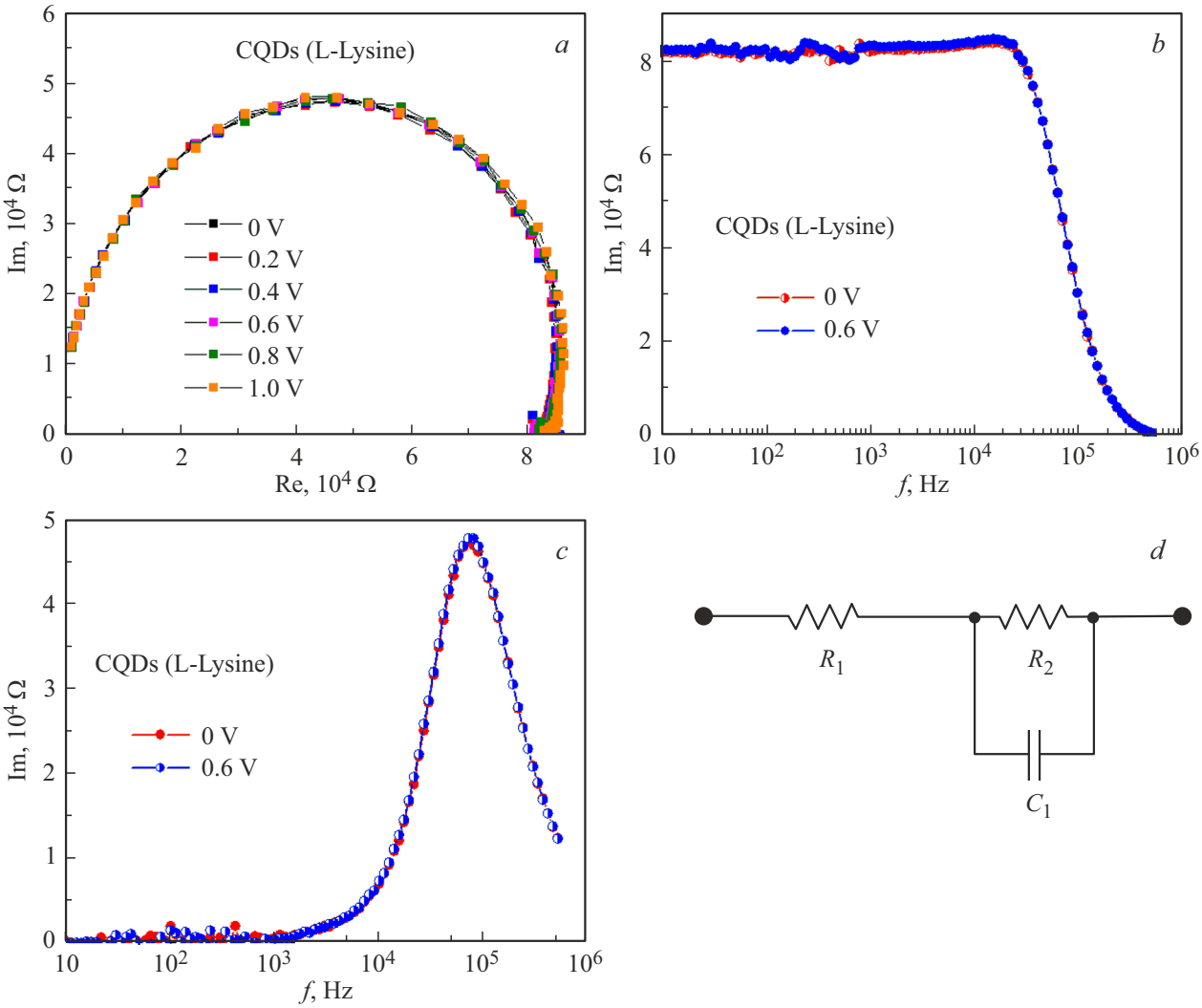

Figure 3. *a*) Impedance of characteristic of CQDs film based on L-Lysine upon application of different voltage; *b*) frequency dependences of real and imaginary parts; (*c*) impedance of characteristic of CQDs film based on L-Lysine; *d*) equivalent scheme of sample of CQDs film based on L-Lysine.

lated root mean square−RMS) with central frequencies 20, 70, 270 and 1000 Hz, $\mathrm{RMS} = [(v_1^2 + v_2^2 + \ldots + v_n^2)/n]^{0.5}$. Fluctuations of short circuit current were calculated as $\delta J = \delta J_{\mathrm{meas}}(1 + R/r)$, where ΔJ_{meas} — is the measured current fluctuations, r — sample resistance. Based on the obtained data, the spectral dependences of the low-frequency noise density on the flowing current and on the frequency were plotted.

3. Results and discussion

Figure 2 shows I-Vs of CQDs film based on L-Lysine, obtained during forward and reverse shift in darkness, and inserts in Figure 2 show distribution of dimensions of CQDs (*a*) and I-Vs of same CQDs film in lg – lg scale (*b*). Figure 2 shows that I-Vs has ohmic nature, and current in the range of voltages from −4 to +4 V follows the law $I \sim V^n$, where $n \sim 1$.

Cole-Cole plots, as well as frequency dependences of real and imaginary part of impedance characteristic for CQDs film of L-Lysine upon application of different voltage, measured in darkness, are presented in Figure 3, *a, b* and *c*.

Arc-like shape of Cole-Cole graph indicates complex impedance behavior of the material, which is typical for materials with heterogeneous conductivity, they include carbon quantum dots. Maximum imaginary part of the impedance is $4.7 \cdot 10^4$ Ω at $f = 4.7 \cdot 10^4$ Ω, this indicates a significant capacity component in the system. This maybe due to the presence of interfacial boundaries and charge traps in the CQDs structure, which is due to their nanometer sizes.

The absence of changes in Cole-Cole graph when changing the bias from 0 to 1 V with step of 0.2 V indicates the high stability of the material in the electric field. This means that CQDs based on L-Lysine have stable electrochemical properties and are stable against voltage

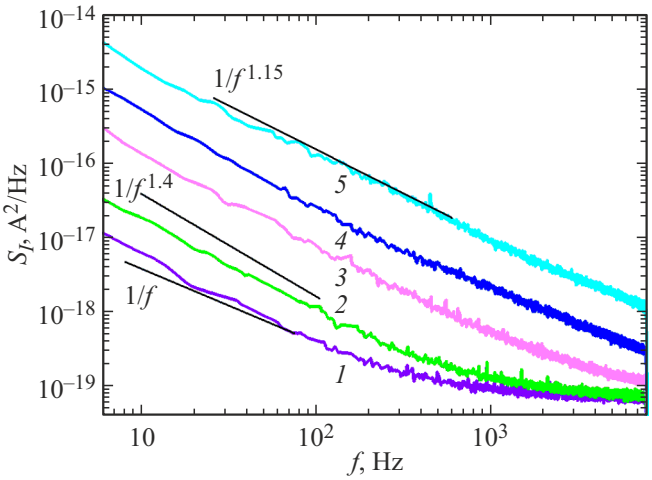

Figure 4. Frequency dependences of density of current noise of CQDs film based on L-Lysine at room temperature at different currents, current I, μA: *1* — 1.2; *2* — 2; *3* — 7; *4* — 16.8; *5* — 39.2.

bias. This fact highlights their potential for use in electronic devices operating under various conditions, such as sensors and memory cells, as well as use in optoelectronic devices such as LEDs and solar cells.

The permanent value of real part of impedance $f < 5 \cdot 10^4$ Hz confirms predominance of resistive component in this frequency range. This is typical of materials where the main resistance is due to the charges movement through the material, and capacitive effects manifest at higher frequencies. The exponential drop of Re at high frequencies indicates the predominance of capacitive behavior, which is due to the decrease in contribution of the resistive component and the increasing role of capacitive effects. This phenomenon is characteristic of materials where the alternating current causes rearrangement of charge states or polarization at interfacial interfaces.

The imaginary part of impedance shows zero values at low frequencies, this means absence of significant capacitive or of inductive effects in this range. Small rise in range from 10^3 to 10^4 Hz can indicate the beginning of polarization processes. Abrupt increase and peak on imaginary part of impedance to 10^5 Hz with maximum value $4.8 \cdot 10^4\ \Omega$ indicates the resonance phenomena. This can be associated with the resonance polarization or inductive effects this confirms the presence of complicated interfacial interactions in the material. Further Im decreasing at frequencies above 10^5 Hz to $10^4\ \Omega$ at $5 \cdot 10^5$ Hz reflects decrease in inductive component and system stabilization.

Cole-Cole plots are in good agreement with the equivalent scheme model (Figure 3, *d*) and represent the series resistance, recombination resistance, and geometric capacitance respectively, which arise due from charge storage, charge transfer resistance, and/or additional interfacial electronic states.

Frequency dependences of density of current noise of CQDs film of L-Lysine at room temperature for different currents are shown in Figure 4. Figure 4 shows that dependences are close to $S_I \propto 1/f^{\alpha}$ $(1 \leq \alpha \leq 1.4)$ noise.

Figure 5, *a* shows the dependences of spectral density of low-frequency current noise on current at room temperature for four analysis frequencies. For frequencies 20 and 70 Hz density of current noise $S_I \propto I^{1.5}$. But for frequencies 270 and 1000 Hz rate of density increasing of current noise reaches $S_I \leq I^{2.5}$. Characteristic deviation of current noise from ideal dependence of Hauge ratio $S_I(I)/I^2 = (\alpha/N)/f$ says that fluctuations of film resistance are not single noise source. Additional contribution can be provided by migration of ions [13]. Ions accumulation at boundaries of grain or globules forms heterogeneities in field distribution and facilitates noise formation [12].

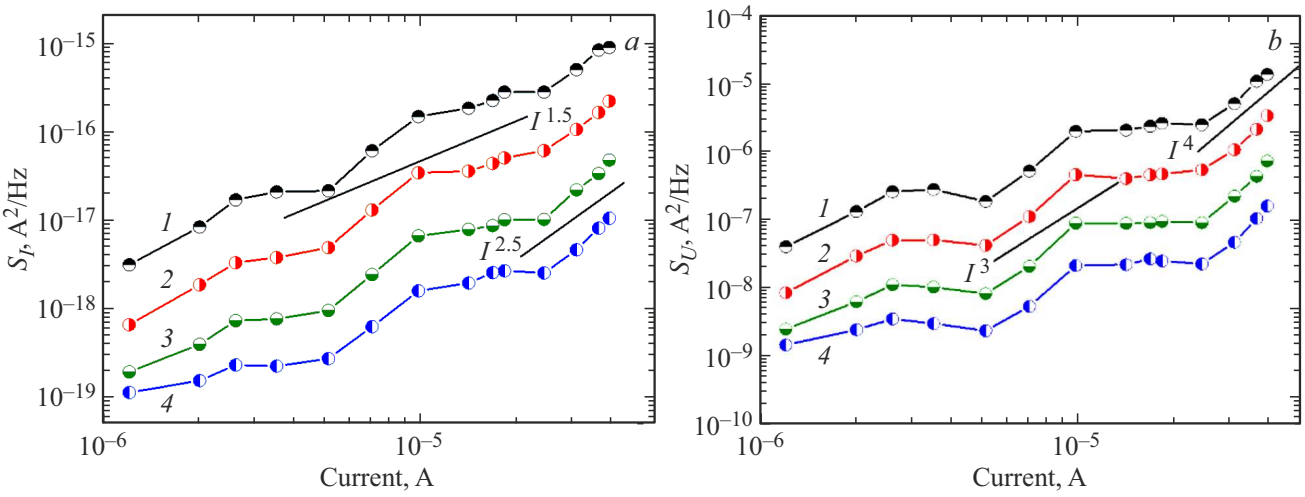

Figure 5. *a*) Density of low-frequency current noise vs. current for CQDs film based on L-Lysine at different frequencies, f, Hz: *1* — 20; *2* — 70; *3* — 270; *4* — 1000. *b*) Density of voltage fluctuation vs. current for CQDs film based on L-Lysine at different frequencies, f, Hz: *1* — 20; *2* — 70; *3* — 270; *4* — 1000.

Nonrepeatability of I-Vs, presence of sections of abrupt increase in noise density $S_I \propto I^{2.5}$ (Figure 5, *a*) for frequencies 270 and 1000 Hz ensure supposition about defects occurrence during current flow, rather of a metastable nature, forming noise associated with their overcharging. More clearly this is expressed in Figure 5, *b* — densities of voltage fluctuations vs. current, where $S_U \propto I^{3.0}$ and even $S_U \propto I^{4.0}$ are observed at individual sections of current dependence. At $I > 20\,\mu$A such a feature is observed for all measurement frequencies 20, 70, 270 and 1000 Hz.

In frequency dependences (Figure 4) $S_I \propto 1/f^{\alpha}$ $(1 \leq \alpha \leq 1.4)$ and this well corresponds to noise $1/f$ or flicker-noise. In Figure 4 white fractional noise or thermal noise independent of frequency in the measurement frequency range are not observed in fact. At $f > 1000$ Hz and currents $\leq 2.0\,\mu$A outsloping of low-frequency noise density occurs at the level of the own noises of the analog-to-digital converter measuring the signal.

We can assume that flicker-noise in CQDs film is associated with oscillations of density of charge carriers (holes and ions) [18], as these measurements, maybe, are due to varying density of carriers as per mechanism of trapping — release [11]. The dependence of density of current noise $S_I \propto I^{1.5}$ supposes competition between recombination noise $(S_I \propto I)$ and noise associated with tunneling of charge carriers using traps $(S_I \propto I^2)$ [19] and impurity states [16] in band gap by hopping conductivity [20], as well as between conducting clusters inside of less conductive array [16]. So, in studied frequency range $(f \leq 8000$ Hz) the flicker-noise is the main one. The obtained results ensure forecast of properties of optoelectronic devices based on CQDs.

4. Conclusion

Dependences of current on applied voltage, low-frequency noise and impedance characteristics of thin films based on CQDs, obtained from L-Lysine using microwave technology, with an average size below 10 nm have been studied. Results of impedance spectroscopy show that Cole-Cole plots are in good agreement with the equivalent scheme model and represent the series resistance, recombination resistance, and geometric capacitance respectively, which arise due from charge storage, charge transfer resistance, and/or additional interfacial electronic states. The physical mechanisms of current flow, current noise formation, and defect occurrence are considered. In studied frequency range $(f \leq 8000$ Hz) noise $1/f$ associated with density oscillations of charge carriers manifest most clearly.

Acknowledgments

The authors are grateful to M.S. Istomina and A.V. Klochkov for their assistance in the synthesis of CQDs based on L-L sine and in the setting of the noise measurement set-up, respectively.

Conflict of interest

The authors declare that they have no conflict of interest.

References

[1] X. Xu, R. Ray, Y. Gu, H.J. Ploehn, L. Gearheart, K. Raker, W.A. Scrivens. J. Am. Chem. **126**, *40*, 12736 (2004).
[2] T. Yuan, T. Meng, P. He, Y. Shi, Y. Li, X. Li, L. Fan, S. Yang. J. Mater. Chem. C **7**, 6820 (2019).
[3] A.R. Nallayagari, E. Sgreccia, R. Pizzoferrato, M. Cabibbo, S. Kaciulis, E. Bolli, L. Pasquini, P. Knauth, M.L. Di Vona. J. Nanostruct. Chem. **12**, 565 (2022).
[4] A. Kim, J.K. Dash, P. Kumar, R. Patel. A.C.S. Appl., Electron. Mater. **4**, *1*, 27 (2022).
[5] B. Vercelli. Coatings **11**, 232 (2021).
[6] N.A.A. Nazri, N.H. Azeman, Y. Luo, A.A.A. Bakar. Opt. Laser Technol. **139**, 106928 (2021).
[7] P. Devi, S. Saini, K.H. Kim. Biosens. Bioelectron. **141**, 111158 (2019).
[8] A. Badawi, S.S. Alharthi, N.Y. Mostafa, M.G. Althobaiti, T. Altalhi. Appl. Phys. **125**, 858 (2019).
[9] G.V. Nenashev, M.S. Istomina, I.P. Shcherbakov, A.V. Shvidchenko, V.N. Petrov, A.N. Aleshin. Phys. Solid State **63**, 1276 (2021).
[10] G. Landi, S. Pagano, H.C. Neitzert, C. Mauro, C. Barone. Energies **16**, 1296 (2023).
[11] C. Barone, F. Lang, C. Mauro, G. Landi, J. Rappich, N.H. Nickel, B. Rech, S. Pagano, H.C. Neitzert. Sci. Rep. 6:34675.
[12] V. Venugopalan, R. Sorrentino, P. Topolovsek, D. Nava, S. Neutzner, G. Ferrari, A. Petrozza, M. Caironi. Chem. **5**, 868 (2019).
[13] V.K. Sangwan, M. Zhu, S. Clark, K.A. Luck, T. J. Marks, M.G. Kanatzidis, M.C. Hersam. ACS Appl. Mater. Interfaces **11**, 14166 (2019).
[14] J. Glemža, J. Matukas, S. Pralgauskaitė, V. Palenskis, Lith. J. Phys. **58**, 194 (2018).
[15] Y. Choi, N. Thongsai, A. Chae, S. Jo, E.B. Kang, P. Paoprasert, S.Y. Park, I. In. J. Ind. Eng. Chem. **47**, 329 (2017).
[16] G.V. Nenashev, R.S. Kryukov, M.S. Istomina, P.A. Aleshin, I.P. Shcherbakov, V.N. Petrov, V.A. Moshnikov, A.N. Aleshin, J. Mater. Sci. Mater. Electron. **34**, *31*, 2114 (2023).
[17] A.M. Ivanov, G.V. Nenashev, A.N. Aleshin. J. Mater Sci: Mater. Electron. **33**, 21666 (2022).
[18] D. Cho, T. Hwang, D.-G. Choa, B.W. Park, S. Hong. Nano Energy **43**, 29 (2018).
[19] L. Li, Y. Shen, J.C. Campbell. Solar Energy Mater.Solar Cells **130**, 151 (2014).
[20] A.M. El'Mahalawy, M.M. Abdrabou, S.A. Mansour, F.M. Ali. J. Mater Sci: Mater. Electron. **34**, 2313 (2023).

Translated by I.Mazurov